

Structural dynamics of (bio-) macromolecules probed by optical spectroscopy

Der Universität Bayreuth
zur Erlangung des Grades eines
Doktors der Naturwissenschaften (Dr. rer. nat.)
vorgelegte Abhandlung

von
Florian Spreitler

aus
Kempten

1. Gutachter: Prof. Dr. J. Köhler
2. Gutachter: Prof. Dr. M. Weiss

Tag der Einreichung: 1.4.16
Tag des Kolloquiums: 26.9.16

Summary

In this thesis, spectroscopic analyses on one biological and one non-biological macromolecular system are presented. In both cases, optical experiments shed light onto the (binding resp. conformational) dynamics of the systems' structure.

The first system under examination was the enzyme CO dehydrogenase (CODH) from the bacterium *Oligotropha carboxydovorans*. Fluorescence correlation spectroscopy was used as a relatively un-complex assay for the confirmation of a binding between enzymes and larger substrates – here, the specificity of the binding of CODH and the cytoplasmic membrane was examined by replacing the binding partners. Instrumentation for further investigations on CODH, especially using time-resolved fluorescence spectroscopy had already been developed, but no agreement with the cooperation partner on the continuation of this line of research could be found. Hence, this instrumentation was further used for the characterisation of a different (non-biological) compound.

This second system was a dimer of two flexibly linked perylene bisimide dyes: di-(perylene bisimide acrylate) – (PerAcr)₂. It served as a model system for higher oligomers resp. polymers containing perylene bisimide, which are candidates for the application in organic solar cells. A combination of spectroscopic techniques was used for the characterization, with time-resolutions down to picoseconds (time-resolved fluorescence spectroscopy resp. anisotropy) and in part with single-molecule sensitivity (fluorescence correlation spectroscopy). By using global analysis methods a description of the measured data with minimised sets of free parameters was pursued, yielding robust hypothesis testing. Additionally, comparisons with molecular dynamics simulations and modelling were conducted. Among other results, it was thus possible to show that the examined dimers change conformation on μs timescales between two aggregated and one isolated state; and that the isolated conformation shows a fast transfer of excitation energy between the two dyes.

The findings were reported in three publications, which are the core of this thesis (chapter 4). In particular the last two publications show a possible way for using poly-(perylene bisimide) in organic solar cells: Instead of relying on the aggregation of the dyes, it should be decidedly avoided and non-coherent energy transfer should be exploited as an efficient transport mechanism.

Zusammenfassung

In dieser Dissertation werden spektroskopische Untersuchungen an einem biologischen und einem nicht-biologischen makromolekularen System vorgestellt. In beiden Fällen konnten anhand optischer Experimente Einblicke in die (Bindungs- bzw. Konformations-) Dynamik der Struktur der Systeme gewonnen werden.

Das erste untersuchte System war das Enzym CO-Dehydrogenase (CODH) aus dem Bakterium *Oligotropha carboxydovorans*. Die Fluoreszenz-Korrelations-Spektroskopie wurde als ein relativ unkompliziertes Verfahren eingesetzt, um Bindungen zwischen Enzymen und deutlich größeren Substraten nachzuweisen – hier wurde die Spezifität der Bindung von CODH und der Zytoplasma-Membran durch Austauschen der Bindungspartner untersucht. Die für weitere Untersuchungen an CODH entwickelte Instrumentierung, insbesondere zur zeitaufgelösten Fluoreszenz-Spektroskopie, wurde zur Charakterisierung eines anderen (nicht-biologischen) System eingesetzt, da mit dem Kooperationspartner keine Einigung über die Fortführung gefunden werden konnte.

Dieses zweite untersuchte System war ein Dimer zweier flexibel verbundener Perylenbisimide: di-(Perylenbisimid Acrylat) – (PerAcr)₂. Es diente als Modell für höhere Perylenbisimid-haltige Oligomere bzw. Polymere, die z.B. Verwendung in organischen Solarzellen finden könnten. Die Charakterisierung erfolgte mit einer Kombination spektroskopischer Verfahren mit bis zu ps-Zeitauflösung (zeitaufgelöste Fluoreszenz-Spektroskopie bzw. Anisotropie) und zum Teil auf Einzelmolekül-Niveau (Fluoreszenz-Korrelations-Spektroskopie). Durch globale Analysemethoden wurde eine Beschreibung der gewonnenen Daten anhand möglichst weniger freier Parameter angestrebt, was robuste Hypothesentests ermöglichte. Auch Vergleiche mit Molekulardynamik Simulationen wurden durchgeführt. So konnte unter anderem gezeigt werden, dass die untersuchten Dimere auf μ s-Zeitskalen zwischen zwei verschiedenen aggregierten und einem isolierten Zustand wechseln und dass im isolierten Zustand ein schneller Energietransfer zwischen den beiden Farbstoffen stattfindet.

Die Ergebnisse wurden in drei Publikationen veröffentlicht, die den Kern dieser Dissertation bilden (Kapitel 4). Insbesondere die Ergebnisse der beiden letzten Publikation zeigen einen Weg auf, wie poly-Perylenbisimid erfolgreich in organischen Solarzellen verwendet werden könnte: Anstatt auf die Aggregation der Farbstoffe zu setzen, sollte diese dezidiert vermieden werden und statt dessen nicht-kohärenter Energietransfer als effizienter Transportmechanismus ausgenutzt werden.

Structural dynamics of (bio-) macromolecules probed by optical spectroscopy

Contents

1	Introduction	1
2	Methods.....	2
2.1	Preparations	2
2.2	Absorption, fluorescence and related effects	3
2.3	Experimental Methods	5
2.3.1	<i>Steady-state spectroscopy</i>	5
2.3.2	<i>Time-resolved fluorescence spectroscopy</i>	5
2.3.3	<i>Fluorescence (Cross-) Correlation Spectroscopy</i>	6
2.3.4	<i>Time-resolved fluorescence anisotropy using a streak-camera setup</i>	6
2.4	Analysis and Simulations	11
2.5	Global analysis of spectroscopic data	12
3	Structural dynamics of (bio-) macromolecules probed by optical spectroscopy .	15
3.1	CODH	15
3.1.1	<i>Potential of fluorescence spectroscopic methods demonstrated by application of FCS to enzyme-membrane interaction</i>	16
3.1.2	<i>Possible further directions of research</i>	17
3.2	(PerAcr) ₂	18
3.2.1	<i>Detection of three distinct conformations from fluorescence correlation and time-resolved spectroscopy</i>	19
3.2.2	<i>Detailed characterisation of (PerAcr)₂ conformations by a combination of time-resolved fluorescence anisotropy and molecular modelling</i>	21
3.2.3	<i>Implications for further research</i>	23
3.3	Summary	25
4	Publications.....	26
5	Bibliography.....	27

1 Introduction

The work that is summarised in this thesis used optical spectroscopy to explore structural dynamics in an enzyme – Carbon-monoxide Dehydrogenase (CODH) from the bacterium *Oligotropha (O.) carboxydovorans* – as well as in a non-biological macromolecule – di-(perylene bisimide acrylate) ((PerAcr)₂). The spectroscopic techniques that were applied range from time-resolved fluorescence spectroscopy and time-resolved fluorescence anisotropy on ensembles to fluorescence correlation spectroscopy, which is inherently a single molecule technique. The experimental results were in most cases compared to analytical models in a global analysis that aimed to minimise number of free parameters. In one case, a parameter-free comparison of models based on molecular dynamics simulations was possible.

The structural dynamics that are examined in this work feature the binding specificity of CODH to the cytoplasmic membrane of *O. carboxydovorans*; the transitions of three different conformations found in (PerAcr)₂; and the hopping of excitation energy in the isolated conformation of (PerAcr)₂, which depends strongly on the exact configuration of the two perylene bisimide dyes involved.

The core of this thesis are the three scientific publications that resulted from these efforts; they are assembled in chapter 4. Chapter 3 gives an overview of the publications, with attention to the interrelations between them. Chapter 2 introduces the applied methods with a spotlight on streak-camera enabled time-resolved fluorescence anisotropy and the global analysis of spectroscopic data.

For details and numerical results the reader is occasionally referred to the original publications in chapter 4; figures, tables and equations are referenced using the following convention: first, the number of the publication is given (1, 2, or 3 in chronological order; cf. the list on page 26), followed by a point and the number of the figure, table, or equation in the corresponding publication (e.g. figure 2.5 refers to figure 5 in publication 2; figure2.SI_1 refers to the first figure in the supporting information of publication 2).

2 Methods

In the following chapter the methods used for sample preparation (segment 2.1), experiments (segment 2.3), as well as analysis and simulation (segment 2.4) are introduced. Where standard techniques were used or the main work was done by collaborators, the description is kept short and the reader is referred to the relevant literature. Textbook-knowledge on the theory of the interaction of light with matter is also only briefly summarised (segment 2.2). A more detailed description of the implementation of time-resolved fluorescence anisotropy measurements (sub-segment 2.3.4) and of the global analysis of spectroscopic data (segment 2.5) is given.

2.1 Preparations

Preparation and purification of CODH and membrane-patches as featured in publication 1 was conducted at the work-group of Prof. Dr. Ortwin Meyer by Dr. Astrid Pelzmann and Brigitte Melzer. Also, the commercially available Xanthine oxidase from bovine milk was transferred into buffer solution by Dr. Astrid Pelzmann. [1] In our lab, both enzyme samples were fluorescently labelled using a commercially available labelling kit. The DOPC and DOPG liposomes were also prepared using a commercially available preparation kit. Stock solutions were kept at -80°C and fresh dilutions were prepared for every experiment.

Preparation and purification of PerAcr and $(\text{PerAcr})_2$ as featured in publication 2 and 3, as well as higher PerAcr oligomers was conducted at the work-group of Prof. Dr. Mukundan Thelakkat by Dr. Michael Sommer. [2, 3] From these preparations, stock solutions in toluene were generated and stored at -20°C ; fresh dilutions were prepared for every experiment.

2.2 Absorption, fluorescence and related effects

All the experimental methods used in this work make use of the fluorescence of the compounds under investigation. The following working definition of fluorescence and related effects of dye molecules in solution at room temperature is used (cf. also figure 1a); note that only the lowest singlet states are considered for simplicity).

In the steady-state the molecule is in its electronic ground-state G . From there, excitation into an excited state E is possible with light of a matching wavelength: the photon energy hc/λ_1 has to be equal to the energy difference between the two states involved. Note that in figure 1a), the electronic states are made up of sub-states; in fact, in the case of molecules in solution at room temperature, there is usually a continuum of states, e.g. vibrational and rotational states interacting with the solvent. A measure for the probability of the absorption of a photon of wavelength λ_1 is $\epsilon(\lambda_1)$, the extinction coefficient or absorption spectrum. After the absorption of a photon, the molecule undergoes relaxation, losing energy to the solvent (grey arrows). One way back to the electronic ground state G is through the emission of a photon with an energy hc/λ_2 equal to the energy difference between the two states involved. This fluorescence process (along with competing non-radiant processes) is probabilistic, leading to an exponential decay behaviour with an average fluorescence lifetime τ . After fluorescence, there is in general another relaxation resulting in a steady state. A measure for the probability that an emitted photon has the wavelength λ_2 is $F(\lambda_2)$, the fluorescence spectrum. Absorption and fluorescence are not isotropic but follow the directional characteristic of the Hertzian dipole for electronically dipole allowed transitions. The transition dipole moment of absorption and emission is closely bound to the molecular scaffold; i.e. the orientation of the molecule determines from which direction and with what polarisation it is most likely to be excited; and the orientation also determines the direction and polarisation of the emitted photon. [4]

If two or more molecules are close to one another, additional effects are possible: For dyes with matching absorption- and fluorescence spectra, resonant energy transfer over distances in the order of some nanometres can take place (weak coupling). A simple model for this effect is the Förster Resonance Energy Transfer (FRET, cf. fig. 1b)): after excitation of one molecule – the donor (states G_D and E_D) – the excitation can be transferred to another molecule – the acceptor (states G_A and E_A). This process – symbolised by the dotted arrows – takes place with a rate k_{FRET} that depends on the distance and orientation of the molecules in addition to their spectroscopic properties. [5] There are also many other mechanisms leading to a loss of excitation energy, collectively called quenching. [6]

Further, two or more molecules of the same type can form aggregates, which leads to different absorption and emission characteristics (strong coupling). In figure 1c), this is shown for two identical molecules with electronic states G and E . The aggregate possesses an electronic ground state with a lowered energy, while there are two new excited states (E_J and E_H) with different energies. Thus the absorption and fluorescence spectra of the aggregate differ significantly from the monomer. Depending on the relative orientation of the components of an aggregate, only certain transitions from the ground state take place upon interaction with light. E.g. in the case of J-aggregates, there is a red-shift of the absorption

spectrum with respect to the un-aggregated spectrum (transition to E_j only); in H-aggregates, the absorption spectrum blue-shifts (transition to E_H only). [7, 8]

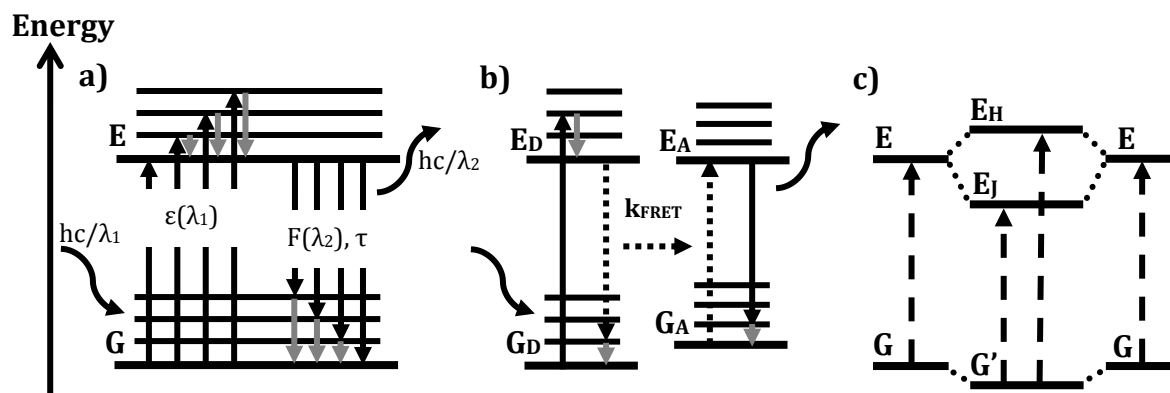


Figure 1: Working definition of fluorescence and related effects of dye molecules. The black arrows symbolise radiant transition between the states (G for electronic ground states, E the lowest excited singlet states), the grey arrows symbolise non-radiant relaxation. a) Jablonski diagram: absorption and emission of light. b) Weak coupling: Förster Resonance Energy Transfer (FRET, indices D for donor resp. A for acceptor molecules). c) Strong coupling: Energy shifts and splitting of excited states of strongly coupled molecules upon aggregation. The arrows symbolising possible excitations are dashed for a better visibility of the differing excitation energies.

2.3 Experimental Methods

This section succinctly introduces the experimental methods used in this work closing with a more detailed description of the implementation of time-resolved fluorescence anisotropy measurements.

2.3.1 Steady-state spectroscopy

The basic characterisation of compounds examined in this work was done on commercial spectrometers (absorption: Perkin Elmer Lambda 9 UV/VIS/NIR spectrometer; fluorescence and fluorescence excitation: Varian Cary Eclipse fluorescence spectrophotometer). The implementation of the measurements of the absorption and fluorescence spectra is straight forward and thus not discussed here. [9] The fluorescence spectrophotometer makes the variation of excitation as well as detection wavelength possible and was thus also used to obtain excitation spectra where a heterogeneity of a sample was suspected (cf. publication 2, figure 2 and the discussion on page 7975). In this case, the absorption spectrum shows only a superposition of the absorption spectra of the components. The measurement of an excitation spectrum resembles that of an absorption spectrum in that the wavelength of the light traversing the sample is varied; but instead of the transmitted intensity, the fluorescence intensity to a certain wavelength region is measured. For a homogeneous fluorescent sample, the two spectra are identical. But if the sample is made up of more than one component with differing fluorescence spectra, the excitation spectrum varies as a function of the chosen detection wavelength.

2.3.2 Time-resolved fluorescence spectroscopy

For the measurement of time-resolved data, a streak-camera setup was implemented. The principle of operation of streak-cameras has been discussed in detail elsewhere and will not be repeated here. [10, 11] The basic premise of streak-camera measurements is the simultaneous determination of 1-dimensional spatial data as well as temporal data. A 2-dimensional image is obtained where the e.g. the horizontal position codes where on the streak-camera cathode the signal was detected and the vertical position codes when the signal was detected with respect to a trigger signal. Because of their transformation of temporal to spatial data, streak-cameras avoid limitations of detector read-out times, yielding temporal resolutions down to ps. In fluorescence spectroscopy, streak-cameras are conventionally combined with an imaging spectrograph, thereby occupying the spatial streak-camera axis with spectroscopic data (cf. figure 2.3 for a detailed example). This enables the measurement of time-resolved fluorescence spectra. Next to the possibility to measure very short fluorescence lifetimes because of the time-resolution afforded by the streak-camera, its main advantage is the possibility to resolve different components in a compound. Assuming a

heterogeneous sample where the components' fluorescence lifetimes differ significantly, it is possible not only to provide evidence of this heterogeneity but to characterise the components with respect to their fluorescence spectrum. The determination of these decay-associated spectra (DAS) is possible using a global analysis approach as introduced in section 2.5. [12]

2.3.3 Fluorescence (Cross-) Correlation Spectroscopy

While the other methods used in this work all examine ensembles of molecules, FCS is a single-molecule technique in that it makes it possible to examine effects that would otherwise be invisible in the ensemble average. [13] FCS works with an extremely small detection volume (in the order of femto-litres) created by a confocal measurement scheme and rather low sample concentrations (in the order of nM) so that only a finite number of molecules (in the order of 10-100) is excited by the laser and contributes to the fluorescence signal. Single-molecule resolution is achieved through the autocorrelation of the signal I (or the cross-correlation, if more than one signal I_n was obtained):

$$G(\tau) = \frac{\langle I_1(t) \cdot I_2(t + \tau) \rangle}{\langle I_1 \rangle \cdot \langle I_2 \rangle} \quad (1),$$

where τ is a lag time and the brackets denote the time average.

Only contributions from correlated events remain in the correlation function G (e.g. one and the same molecule diffusing in and out of the detection volume), while all contributions from non-correlated events are suppressed (e.g. two molecules coincidentally diffusing out of the detection volume at the same time). Comparing the obtained correlations curves to analytical models, a broad range of questions can be addressed. A basic effect to be observed in liquid samples is the decay of the autocorrelation curve in dependence on the diffusion coefficient (and thus, the size) of the components of the sample. This effect is used in publication 1 to determine whether binding between different probes and substrates takes place; the author was assisted in the acquisition of the FCS data in publication 1 by Dr. Christian Brock. In publication 2 the conformational dynamics of (PerAcr)₂ are examined, e.g. by analysing the switch from green to red fluorescence on one and the same molecule by a 2 colour cross-correlation experiment.

2.3.4 Time-resolved fluorescence anisotropy using a streak-camera setup

As already mentioned above, absorption and fluorescence are both linked to the orientation of the molecules through the corresponding transition dipole moments. Illuminating an isotropic sample solution with a light pulse of a given polarisation selectively excites those molecules that are oriented favourably, i.e. whose transition dipole moments

are close to parallel to the excitation polarisation: the sample is now anisotropic (cf. figure 2). This anisotropy and its decay by e.g. rotational diffusion can be determined by comparing fluorescence signals with parallel and perpendicular polarisation (I_{\parallel} resp. I_{\perp}) with respect to the excitation light:

$$r(t) = \frac{I_{\parallel}(t) - I_{\perp}(t)}{I_{\parallel}(t) + 2 \cdot I_{\perp}(t)} \quad (2)$$

The anisotropy, r , decays mono-exponentially with a correlation time θ for a spherical molecule undergoing only rotational diffusion (depending on its size, the viscosity of the solvent and the temperature). $r=0$ for isotropic emission (e.g. after rotational diffusion has “deleted” the anisotropic distribution of excitation); for detection directly after excitation (i.e. before effects like rotational diffusion), $r = 0.4$ if the transition dipole moments are parallel and $r = -0.2$ for perpendicular transition dipole moments. More details can be found in publication 3 and in literature. [14] The impact of fluorescence anisotropy on measured fluorescence signals can be suppressed by adjusting the angle between excitation and fluorescence polarisation to the “magic angle” of 54.74° .

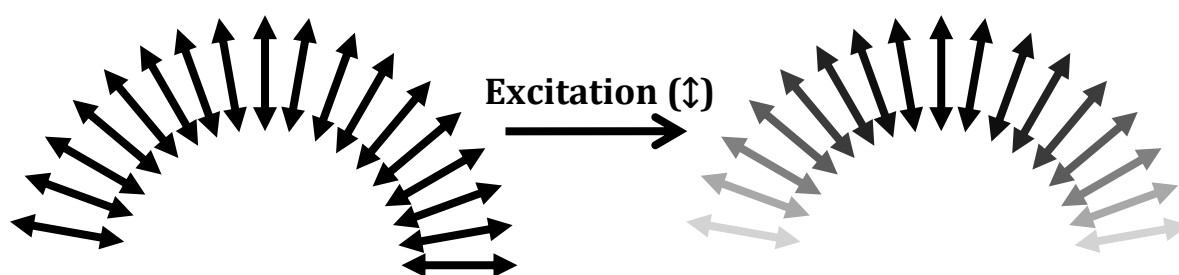


Figure 2: Generation of anisotropy by excitation with linearly polarised light. Transition dipoles / molecule orientations are symbolised by the double arrows (the third dimension is omitted for simplicity). In an isotropic sample, all molecule orientations have the same probability (left hand side). After excitation with vertically polarised light, orientations that are near to vertical have a higher probability to be in the excited state (right hand side, probability of excitation is symbolised by a grey scale), the formerly isotropic sample is anisotropic.

The imaging spectrograph in the streak-camera setup implemented in this work allows an automated switch between the monochromator grating and a mirror originally designated for adjustment. Together with some alterations to the conventional streak-camera setup for fluorescence spectroscopy this was used to implement a setup for time-resolved fluorescence anisotropy.

The design goal was to enable the simultaneous measurement of the two relevant polarisation directions of the sample emission: parallel and perpendicular with respect to the polarisation direction of the excitation. In the implementation at hand, this anisotropy resolution comes at the cost of spectral resolution, but it has to be noted that a combination

of both is conceptually straight forward (cf. the short discussion on this topic at the end of this section). Below, the basic idea and the actual implementation of the anisotropy setup is discussed, followed by an example of streak image generated with this setup and the subsequent extraction of data.

Given that the streak-camera cathode acts as a line-detector the only challenge concerning polarisation resolution is the generation of two separate images of a given light source with mutually perpendicular polarisation (for now, the light source can be considered to be a point source). A possible solution for this problem is shown in figure 3a): the light from the source (depicted as a beam for simplicity) is split by a polarising beamsplitter. Each of the two resulting beams of mutually perpendicular polarisation is then deflected onto a second polarising beamsplitter by a mirror. Since the beam that is reflected by the first beamsplitter is also reflected by the second one (and correspondingly for the transmitted beam) both beams leave the system in the same general direction. But it is now possible to independently adjust the exact direction of the two beams by turning the two mirrors, thus generating two beams of mutually perpendicular polarisation propagating with a small angle among each other. From the direction of the streak-camera, the source has been split into two virtual sources that are consequently imaged onto different spots of the streak-camera cathode.

The implementation of this idea into a setup for time-resolved fluorescence anisotropy is shown in figure 3b); details about the used components can be found in publication 3, page 25960. The excitation light is generated by a combination of a pulsed Ti:Sa laser, a pulse picker and a frequency doubler (as well as a filter to clean out residual first harmonic radiation) followed by a combination of a half-wave plate and a linear polariser that allow the adjustment of a linear polarised excitation oriented vertically in the laboratory coordinate system for the anisotropy experiment. The excitation pulses are focussed into the sample cuvette and the generated emission is collected under right-angle conditions. The signal is then to be steered towards the streak-camera using the beamsplitter / mirror system explained above. But before that, a further optical system needs to be included in the detection path: because of the right angle detection and the finite dimensions of the cuvette, the light source is not a point source; as a first order approximation, it has to be treated as a line-source. The adjustment of the lateral extent of this line-source is enabled by the generation of an intermediate image on a variable vertical slit. As a consequence, the light from the sample is optically transformed into two virtual line-sources of adjustable extent (1) and independently adjustable position (2,3); these three degrees of freedom are shown by the numbered double-arrows. One of the sources represents the component of the emission with parallel polarisation with respect to the excitation polarisation, the other represents the perpendicular component. Using a dielectric filter, light from the desired spectral region is chosen and focussed into the entrance slit of a combination of an imaging spectrograph and a streak-camera. Because spectral sensitivity is not needed in this case, the spectrograph is used with a mirror instead of a grating; consequently, the width of the entrance slit can be set to the maximum possible value (in principle, the spectrograph itself could be replaced by a mirror, but this solution makes uncomplicated switching to other modes of operation of the streak-camera possible).

Figure 3c) shows an example of the resulting streak-camera image. On the horizontal axis, notice the resolution of the two directions of polarisation (with respect to the

polarisation of the excitation). The vertical axis corresponds to the time after the excitation pulse, and the emission intensity is given by a colour scale, where black / purple represents low intensity and yellow / red represents high intensity. The solid and dashed boxes indicate the perpendicular resp. parallel signals. The impact of the three degrees of freedom of adjustment is depicted by the numbered double arrows: by adjusting the width of the variable slit, the horizontal size of both signals can be changed (1; white arrows; one of the arrows is dotted to symbolise that no independent adjustment is possible); slightly turning the mirrors allows for the horizontal positioning of the corresponding signal on the streak image (2,3; black arrows); Optimal adjustment includes maximisation of the horizontal size of the signals while ensuring sufficient separation and preventing that parts of the signals are clipped by the entrance slit of the imaging spectrograph.

For further analysis, the streak-camera image is integrated along the horizontal axis to generate the two time-resolved signals as shown in figure 3d): the fluorescence components with parallel / perpendicular polarisation with respect to the polarisation of the excitation. The time-resolved anisotropy experiments in publication 3 were conducted using the setup detailed above.

This setup was implemented in a way that makes a switch to the standard mode of streak-camera-enabled time-resolved fluorescence spectroscopy possible: for this, the excitation polarisation is adjusted to the “magic angle” with respect to the vertical axis in the laboratory coordinate-system; the variable slit is opened, so that it has no effect on the detected light; the lower (horizontal) path of the beamsplitter / mirror system is blocked; the detection filter is removed; the entrance slit of the imaging spectrograph is set to a width suitable for spectroscopic measurements; and finally the mirror inside the spectrograph is replaced by one of the two available gratings (the replacement of the gratings and mirrors is an automated feature of the spectrograph). The time-resolved spectroscopy experiments in publication 2 were conducted using this modified setup.

In principle a combination of the two modes – spectral resolution as well as resolution of anisotropy in one measurement – is possible with only minor changes to the anisotropy setup. In this case, the variable slit would be set to a small width to act as an effective entrance slit of the imaging spectrograph; the dielectric filter in front of the streak-camera would need to be replaced by a filter with a dedicated bandwidth (see below); the mirror inside the spectrograph would be switched to the corresponding grating (see below). This setup could generate separate spectra of the two anisotropic components of the sample emission on the streak-camera cathode, assuming proper design and adjustment. The design challenge of this setup would be that the variable slit cannot be used to prevent the overlap of the two components like in the anisotropy setup without spectral resolution. This task of ensuring that both spectra fill each less than half of the streak image would fall to a dedicated bandpass-filter that would need to be chosen with respect to the desired grating. With the set of gratings at hand, the greatest width of the bandpass would be approximately 80nm, but given the installation of a grating with a lower line-density, even greater spectral regions could be characterised simultaneously in one and the same anisotropy resolved experiment (for the compounds examined in this work, a 3 to 4 times wider bandpass would be optimal). It has to be noted that a proof of principle of this idea has not been conducted yet.

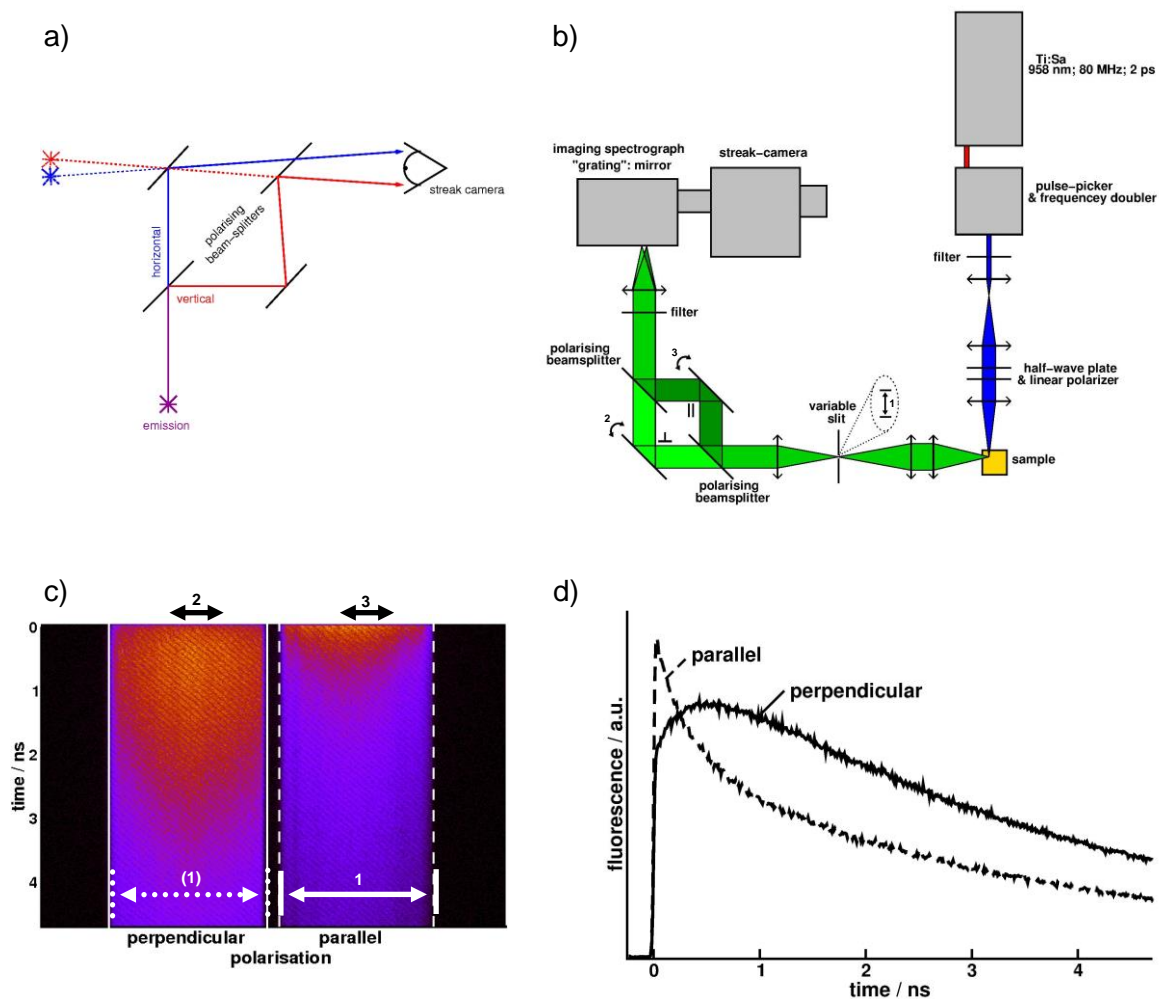


Figure 3: Implementation of a streak-camera based setup for time-resolved fluorescence anisotropy. a) Principle for the optical conversion of a light source into two separate virtual light sources with mutually perpendicular polarisation by use of two polarising beam splitters. b) Setup implemented for the anisotropy experiments in this work. Notice the three degrees of freedom necessary for the adjustment of the anisotropy part of the experiment, as shown by the numbered double arrows. c) Example of the streak-camera image. Notice the resolution of the two directions of polarisation on the horizontal axis (with respect to the polarisation of the excitation). The vertical axis corresponds to the time after the excitation pulse, and the emission intensity is given by a colour scale, where black / purple represents low intensity and yellow / red represents high intensity. The solid and dashed boxes indicate the perpendicular resp. parallel signals. The impact of the possible adjustments from panel b) is depicted by the black and white numbered double arrows (1: optimisation of the size of the virtual images and 2,3: positioning of the two signals on the streak cathode). d) Anisotropy resolved fluorescence decays of the sample emission that results from integration of the streak image along the horizontal axis within the two intervals marked in panel c).

2.4 Analysis and Simulations

This work uses experimental data to test hypotheses about the compounds under investigation. In general, the scientific method is an iterative procedure, where a hypothesis is formulated, its conformity with the experimental evidence is judged and depending on the outcome the hypothesis is retained or refused. In case of a refusal, a new iteration starts with the formulation of a new or modified hypothesis.

Three different approaches to the formulation of hypotheses were chosen. In some cases, the hypothesis was a qualitative statement about the expected outcome of an experiment (cf. publication 1). In one case a theoretical simulation with subsequent modelling yielded an expected outcome that could be compared to the outcome of the actual experiment. In this case of a quantitative comparison of model and experiment, the numerical model did not feature any free parameters (cf. publication 3). Most of the data in this work were analysed using an analytical model of the expected outcome of the experiment with a number of unknown free parameters. This model was then fit to the entire dataset at once by a non-linear least squares algorithm and subsequently judged for its accuracy in describing the experimental data. Again, depending on this judgment, the model was either retained or refined. This third approach – termed global analysis in the following – is introduced in more detail at the end of this chapter. In all three cases the comparison of the modelled outcome with the actual experiment was conducted by a visual comparison of the curves, with consideration of the noise-level of the experiment.

The non-linear least squares fits were conducted using the freely distributed software gnuplot (for the exact version cf. the respective publications). It incorporates a Levenberg-Marquardt algorithm for non-linear optimisation problems and was chiefly chosen for its flexibility concerning the definition of complex model functions. In one case (cf. publication 2) the model function was derived using the computer algebra system Maple (version 13).

Molecular dynamics simulations and further modelling in publication 3 was conducted at the work-group of Prof. Dr. Stephan Gekle by himself and Moritz Hollfelder. [3]

2.5 *Global analysis of spectroscopic data*

Experiments like the ones in section 2.3 generate data that can be interpreted as a set of curves – one observable as a function of one variable (e.g. the measured fluorescence intensity as a function of time after the excitation pulse: fluorescence decays) – depending on one or more further parameters (e.g. detection wavelength, polarisation). The principles used in this work concerning the global analysis of such data are discussed in this section. The section starts with an enumeration of the different sorts of datasets that were analysed as a part of this work (for details cf. the corresponding publication), followed by a general description of the global analysis approach chosen as a means of testing hypotheses concerning the compounds under investigation.

The anisotropy setup introduced in the preceding section generates two anisotropic fluorescence decays per measurement. In publication 3, two such measurements were conducted on one and the same sample with different spectral ranges as defined by the detection filters used. The resulting dataset is a set of four fluorescence decays with the spectral detection range and the polarisation as additional parameters. An analysis of such data has to cope with “bookkeeping” parameters like e.g. background signals and onset times of the different curves; it allows the determination of physical parameters like anisotropy decay times; and it can be used to test hypotheses about the compound under investigation like e.g. “The transition dipole moments of absorption and fluorescence of the only component are parallel”.

In publication 2, three FCS measurements on one and the same sample were conducted: two auto-correlation measurements of the signal in different spectral regions and a cross-correlation measurement between the two spectral regions. An analysis of such data has to cope with “bookkeeping” parameters like e.g. the number of molecules in the detection volume and diffusion times that possibly differ from curve to curve; it allows the determination of physical parameters like the populations of different conformations; and it can be used to test hypotheses about the compound under investigation like e.g. “The compound consists of one component that dynamically changes between two conformations”.

An extensive number of datasets results if streak-camera based measurements deliver truly two-dimensional data: in publication 2 time-resolved spectroscopy measurements were repeated on one and the same sample with a variation of the detection wavelength interval and the time resolution. The resulting dataset is a set of well over one hundred fluorescence decays with the detection wavelength and the time resolution as additional parameters. An analysis of such data has to cope with “bookkeeping” parameters like e.g. the absolute fluorescence intensity and the width of the instrument response function; it allows the determination of physical parameters fluorescence decay times and fluorescence spectra; and it can be used to test hypotheses about the compound under investigation like e.g. “The compound consists of two emitting species”.

The examples above share the common feature that the data-analysis deals with a number of parameters that can be again classed into two categories: First, the “book-keeping” parameters are not a property of the sample but e.g. a function of the used equipment or the

total measurement time. They need to be incorporated into the model describing the dataset as either known or free parameters but are typically independent of the exact nature of this model (e.g. the background intensity of a time-resolved fluorescence curve needs to be considered irrespective of the number of exponential decays that are assumed). Second, the physical parameters are properties of the compound under investigation. As opposed to the “bookkeeping” parameters neither their number nor their exact nature is necessarily known at the start of the analysis, since they depend on the exact model that is used to try to describe the dataset. In this work, generally only the physical parameters are reported.

Both sorts of parameters can also be classified with regard to whether they only influence one of the measured curves, or some or even all of the curves. A visualisation for this is shown in the Venn-diagram in figure 4. It symbolises a hypothetical experiment consisting of three measurements (e.g. fluorescence decays of a dye measured at three different detection wavelengths). A model describing the experiment would consist of parameters that are needed to describe all three of the curves (global parameters A_n ; e.g. the sum of the absolute measured intensities, fluorescence lifetimes), one curve (local parameters E_n, F_n, G_n ; e.g. relative amplitudes, contribution of scattered light), or possibly some, but not all of the curves (partially global parameters B_n, C_n, D_n ; this could e.g. be the case if one component of the sample shows only negligible fluorescence at one of the used detection wavelengths).

Based on the above considerations the following iterative procedure has been used to analyse most of the experimental data that make up this work.

- Hypothesis: Based on previous knowledge about the compound and previous iterations (if applicable), the most basic hypothesis about the sample is formulated.
- Analytical model: An analytical model is formulated that describes the measured quantity. The generation of the model is not mathematically motivated, but directly influenced by the hypothesis. Explicit and implicit assumptions contained in the hypothesis are explicitly modelled to minimise the number of free parameters while maximising the subset of global or partially global parameters.
- Optimisation: A least squares algorithm is used to obtain the optimal values for the free parameters of the analytical model. For the complete data-set at once, the difference between model and experiment is minimised; where possible, the data-points are weighted according to their error level.
- Accept/ refuse: The optimised model is compared visually to the experimental data. If the comparison is negative, i.e. model and experiment do not match within the experimental error, a new iteration with a refined hypothesis is necessary. In the case of sufficient correlation, the hypothesis is adopted and the physical parameters are thought to provide valid information about the sample. Of course, later experiments can retroactively prove the hypothesis false, triggering a restart of the process.

As an example, consider a streak-camera based time-resolved fluorescence experiment of a previously unknown sample (n fluorescence decays detected at different wavelengths). The most basic hypothesis in this case is: “The sample contains exactly one component that

shows normal absorption and fluorescence behaviour”, i.e. the component follows the working definition of fluorescence (cf. section 2.2). A purely mathematical approach to modelling this experiment would assume n independent exponential decays, yielding $2n$ free parameters (n amplitudes, n decay times; bookkeeping parameters are not considered in this example for simplicity). Aiming for generality, the mathematical approach could possibly even initially start by modelling $m > 1$ exponential contributions per decay, thus generating a model using $2mn$ free parameters. Staying true to the hypothesis (“one component, normal fluorescence”), the suitable model would contain n mono-exponential decays that all share the same fluorescence lifetime as a global parameter, yielding only $n+1$ free parameters (n amplitudes, 1 decay time). After optimisation, the comparison of model and experiment would either be positive. In this case, the fluorescence lifetime of the sample as well as its fluorescence spectrum has been determined (spectra acquired in this way are called decay associated spectra (DAS)). A negative comparison, on the other hand, would make a refinement of the hypothesis necessary. E.g. an additional component the sample could be postulated.

The advantage of the maximisation of (partially) global parameters in the analytical model while minimising the total number of parameters is twofold. On the one hand, the model is more robust and thus the least-squares algorithm while converge faster. In this way, even rather complex models are possible with a reduced risk of producing arbitrary results for the free parameters. On the other hand, the model is less flexible and it is thus possible to detect even subtle flaws in the hypothesis. That way, a hypothesis that was tested positively and its associated parameters are more reliable. [12]

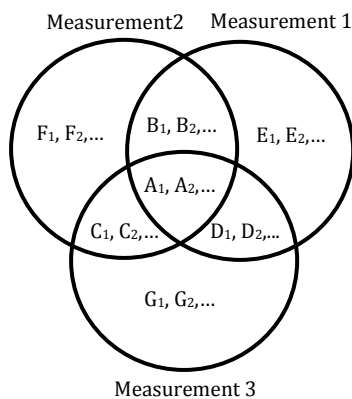


Figure 4: Venn-diagram symbolising a hypothetical experiment consisting of three measurements (e.g. fluorescence decays of a dye measured at three different detection wavelengths). An associated model would use global (A_n), partially global (B_n, C_n, D_n) or local parameters (E_n, F_n, G_n).

3 Structural dynamics of (bio-) macromolecules probed by optical spectroscopy

In the following sections the three publications that are the core of this work are introduced. These sections are intended as an overview of the key results and the approaches taken to reach them; the aim is also to show interrelations between the publications. The publications are addressed in chronological order of appearance to reflect the growing understanding of the biological and chemical compounds under investigation on the one hand and the growing sophistication of the applied experimental and analytical techniques on the other hand. For details and numerical results the reader is referred to the original publications in the next chapter; in many cases, references to figures, tables or equations from the publications are given, using the following convention: first, the number of the publication as established below and in the next chapter is given, followed by a point and the number of the figure, table, or equation in the corresponding publication (e.g. figure 2.5 refers to figure 5 in publication 2; figure2.SI_1 refers to the first figure in the supporting information of publication 2).

3.1 CODH

Oligotropha (O.) carboxydovorans is a soil bacterium found e.g. in coal seams, whose metabolism can utilise carbon monoxide, next to other substrates (i.e. it can “breathe” CO.). A catalyst for the corresponding reaction is the enzyme carbon monoxide dehydrogenase (CODH in the following). [15]

CODH is a member of the large family of flavo-enzymes, which all have a flavin (flavin adenine dinucleotide – FAD or flavin mononucleotide – FMN) as a common co-factor, i.e. the flavin is a non-protein component of these enzymes that is necessary for their function. [16, 17] In CODH, FAD is thought to be an integral part of the reduction and oxidation processes that drive CO-respiration. [18]

Since FAD is also a fluorescent dye, spectroscopic studies of its properties in CODH promised valuable insights into its role in the CO-respiration, using the dye a reporter on changes its immediate environment. E.g. there is a tyrosine amino acid in the vicinity of FAD, which quenches its fluorescence (making it de facto non-fluorescent) but could also play a role in CODH’s function. [19] Because of this heavy quenching, especially time-resolved experiments were planned to shed light on the time-scales involved.

Another feature that lent itself to be examined by fluorescence spectroscopy is the binding of CODH to the cytoplasmic membrane of *O. carboxydovorans*, the amount of CODH bound to the membrane being the rate-limiting factor for respiration. [20]

3.1.1 Potential of fluorescence spectroscopic methods demonstrated by application of FCS to enzyme-membrane interaction

The starting point for publication 1 was the question of the specificity of CODH-binding to its cytoplasmic membrane. While this binding had been shown to be specific in the late 1980s, the corresponding experiments had been rather indirect – the amount of CO-respiratory activity of was used as a means of comparing CO-grown bacteria to others that had been grown in absence of CO. [21] In principle this old experiment could only prove that bacteria grown in a CO-free environment showed no respiratory activity, a specific proof for the inhibition of binding was missing.

This was seen as a welcome possibility to demonstrate the power of fluorescence-based techniques in general and specifically FCS for the study of subcellular biological questions. Since FCS is sensitive to the physical size of the particles under investigation, the question whether a binding between a small molecule (probe) and a much larger compound (substrate) takes place can be straight forwardly answered: if the FCS-curve of the mixed solution resembles that of a probe-only solution, no binding takes place. If the FCS-curve shifts or – more generally – adopts features from the substrate-only solution, a binding takes place. An example of this principle is the proof of successful labelling of CODH with fluorescein (cf. figure 1.1). Here, the FCS-curve of the mixture is shifted on the time-scale by one order of magnitude with respect to the fluorescein-only sample, with no detectable unbound fluorescein residue.

The binding specificity between a probe and a substrate has to be viewed from two perspectives. First, does the probe accept deviating substrates; and second, does the substrate accept a replacement of the probe? The original probe-substrate pair was CODH and a sample of patches of the cytoplasmic membrane of CO-grown *O. carboxydovorans*. Because CODH is de facto non-fluorescent, it had to be fluorescently labelled with fluorescein to be detectable by FCS; the membrane patches on the other hand yielded a sufficient signal, presumably from Raman-scattering. As alternative substrates, artificial receptor-free membranes – unilamellar liposomes prepared from 1,2-dioleoyl-sn-glycero-3-phosphocholine (DOPG) and 1,2-dioleoyl-sn-glycero-3-[phospho-rac-(1-glycerol)] (DOPC) – were used while additionally varying the NaCl-concentration. As an alternative probe, fluorescein-labelled Xanthine Oxidase from bovine milk (XO) was applied; this enzyme resembles CODH in many ways, most notably in its overall 3D-structure.

Mixing the original probe (CODH) with the original substrate (patches of cytoplasmic membrane) yielded a positive result: the features of the FCS-curve from the substrate-only sample were reproduced in the probe-substrate measurement, cf. figure 1.2. All other combinations – CODH vs. alternative substrates as well as the alternative probe XO vs. patches of cytoplasmic membrane – yielded negative results: no change in the FCS-curves could be detected, cf. figures 1.4 and 1.5.

The range of applied alternative substrates and NaCl concentrations with a negative binding result allows to eliminate the possibility of unspecific binding though hydrophilic or hydrophobic interactions as well as electrostatic interactions. The negative binding result of

XO suggests that the binding of CODH to its cytoplasmic membrane has more subtle prerequisites than a comparable 3D-structure. Thus, the hypothesis of a dedicated key-lock pair of receptors governing this binding was not falsified.

It has to be noted, though, that the comparison made in the original publication – the comparison between CO-grown bacteria and bacteria grown in a CO-free environment – has not been repeated in this study. The study serves as a proof of principle of FCS as a direct and relatively un-complex assay for testing hypotheses about the binding behaviour of CODH to its cytoplasmic membrane.

3.1.2 Possible further directions of research

In fact, the logical next step concerning the binding behaviour of CODH would have been the preparation of CODH and patches of cytoplasmic membranes from *O. carboxydovorans* grown under CO-free conditions and using the FCS assay to compare all four probe-substrate pairs made possible by this new preparation and the one already at hand: both versions of CODH vs. both versions of membranes. Thus, the hypothesis that CODH only binds to the membrane of CO-grown bacteria could be directly tested and more details could be revealed: do both the membrane and the enzyme miss their receptors in *O. carboxydovorans* grown under CO-free conditions or does CO-free growth affect only one part of the pair?

From this and from other sources possible receptors in CODH and the cytoplasmic membrane could be identified and selectively “switched off” by the generation of mutated species or other means. Then, CODH-binding could be investigated in great detail using the FCS-assay demonstrated in publication 1.

The examination of CODH on a more microscopic scale in the scope of this work had also already been prepared in parallel to the FCS studies. A streak-camera based experiment for the time-resolved measurement of the fluorescence emitted by the FAD cofactor of CODH was set up and operational: time-resolved spectra from FAD-, CODH- and XO-solutions down to a temporal resolution of 2 ps are available; first tests on a CO-enriched CODH-solution showed significant spectral shifts and an increase in fluorescence quantum yield. [22] A completion of these datasets would require the preparation of further samples, most notably mutants of CODH. For example, the examination of a CODH-mutant lacking the FAD-neighbouring tyrosine would allow to study the role of tyrosine in the quenching of FAD in CODH on the one hand and its role in the respiratory function of CODH.

Unfortunately, the mutants and preparations referred to in the preceding paragraphs could not be provided, as the cooperation partner was unwilling to continue this line of research.

On the other hand, current questions in the field of organic solar cells could obviously be tackled using equipment and know-how already established or in preparation. This led to a switch of the focus of this work.

3.2 (PerAcr)₂

One idea to optimise the efficiency of organic solar cells – and thereby make their actual implementation outside of academic research more attractive – is the introduction of a favourable structure with respect to charge transport while keeping with one of the key advantages of organic solar cells – their printability. This triggered approaches to use self-assembling polymers in organic solar cells. One attempt by Thelakkat et al. made use of the inherent property of many perylene bisimides (PBI) to form potentially large aggregates. They developed block-co-polymers where one part carries a PBI on every repeat unit, thereby providing an electron donor with a tendency for crystallisation; the other part consists of an electron acceptor and is thought to favour the amorphous phase. Indeed it could be shown that a self-assembly into worm-like chains is possible, but concerning the performance as a solar cell, the compound did not show a significant boost. [23, 24]

One suggested reason for this less-than-expected performance was that the physical properties of the PBIs are e.g. changed by aggregation. Since the instrumentation already implemented as part of this work was deemed useful for investigations into changes of the electronic state of the aggregated PBIs it was used as the starting point of a collaboration to improve the understanding of aggregation in PBI polymers.

To decrease complexity, only the PBI part of the aforementioned block-co-polymers was tackled in contrast to the full block-co-polymers. Each repeat unit consists of a PBI unit bound to an acrylate backbone by an undecylalkyl linker, the polymers were thus labelled poly-(perylene bisimide acrylate), shortened as (PerAcr)_n in this work. The structures of PerAcr and (PerAcr)₂ are shown in figure 5. Preliminary experiments on already existing long (PerAcr)_n polymers ($n \gg 100$) confirmed the potential of fluorescence spectroscopy for new insights into these systems. [22] As a systematic approach, a series of short (PerAcr)_n oligomers was prepared ($2 \leq n < 15$), with the dimer preparation reaching de facto mono-dispersity. Especially the transition from monomers to dimers promised insight into the fundamentals of poly-(PerAcr), and is thus the focus of the remainder of this work.

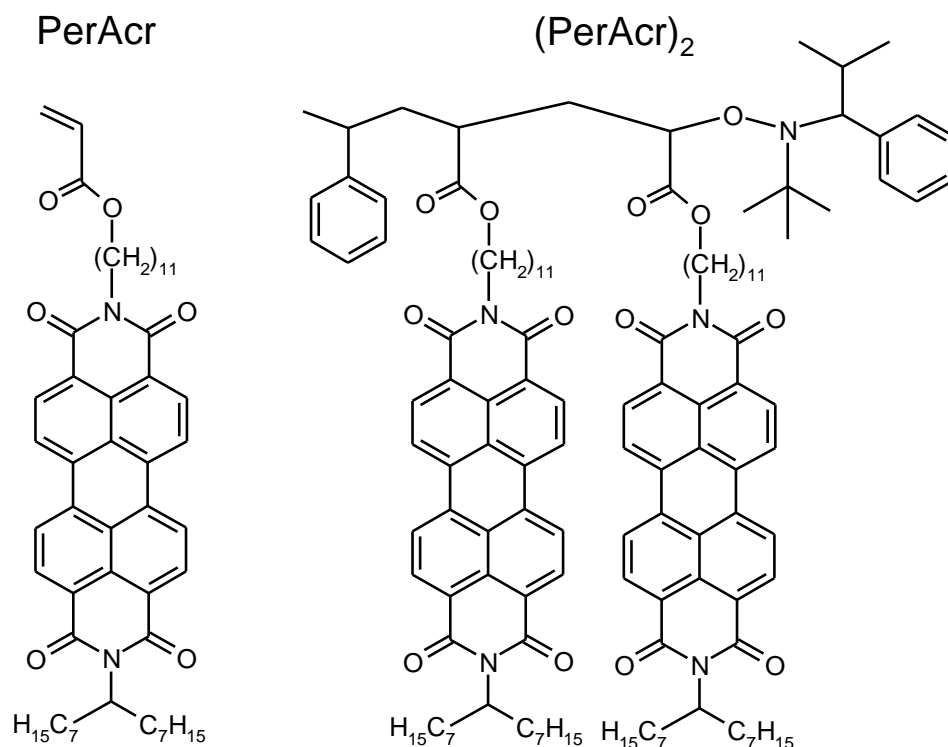


Figure 5: Chemical structures of monomeric and dimeric perylene bisimide acrylates PerAcr and (PerAcr)₂, respectively.

3.2.1 Detection of three distinct conformations from fluorescence correlation and time-resolved spectroscopy

The characterisation of the spectral properties of the (PerAcr)₂ dimer was done in comparison to the PerAcr monomer (dimer resp. monomer in the following). After the first step, a characterisation of both compounds by steady-state spectroscopy, there were already hints that the dimer sample contained two emitting species. As can be seen in figure 2.2, the dimer absorption shows a net shift to the blue (figure 2.2 a)), its fluorescence a net shift to the red (figure 2.2 b)). The series of excitation spectra in figure 2.2 c) shows a dependence of the excitation spectrum on the detection wavelength, which means that more than one species contribute to the signal; the number of emitting species could be identified to equal 2, because the series of excitation spectra features isosbestic points – excitation wavelengths where all different excitation spectra cross. For each of the two species, an absorption spectrum was determined from the excitation spectra, cf. figure 2.5.

The determination of corresponding emission spectra required the application of time-resolved spectroscopy: by a series of measurements over nearly the complete visible wavelength range and four orders of magnitude on the time-scale, fluorescence decay times

of the two emitting species as well as corresponding fluorescence spectra were determined (from decay associated spectra, cf. figure 2.6). Considering the absorption and emission spectra and the fluorescence decay times, one species found in the dimer resembles the monomer very closely; thus it was thought to represent an arrangement where the two PBIs are isolated from each other and thus labelled ISO-(PerAcr)₂. The other species features a blue shifted absorption spectrum, a featureless red-shifted fluorescence spectrum and a fluorescence decay time increased by a factor of 7 with respect to the monomer. Since all of those are features commonly reported for π-π aggregated aromats, the second species was labelled AGG-(PerAcr)₂. Further, a residual signal in the time-resolved experiments hinted at the existence of one or more additional processes/ species with fluorescence occurring on timescales below the experimental time resolution. Barely detectable in the time-resolved experiment, they could be assumed to be de facto non-fluorescent and thus invisible in other optical experiments.

This assignment allowed for two hypotheses about the character of the different species in (PerAcr)₂: either, the heterogeneity of the compound stems from truly different molecules – e.g. isomers – that could be separated by a specialised preparation. The possibility of an extreme example of this case – residual monomer in the dimer preparation – could be eliminated by MALDI-TOF experiments, cf. figures 2.SI-2 and 2.SI-3. Alternatively, the species could co-exist as conformations of one and the same molecule in a steady-state of conformational dynamics.

Since FCS is inherently a single-molecule technique, the logical next step was a systematic three-part FCS experiment on (PerAcr)₂: for both emitting species a corresponding wavelength range was defined using dielectric filters transmitting predominantly the fluorescence of the respective species (green / red wavelength range for ISO-(PerAcr)₂ / AGG-(PerAcr)₂; cf. the summary of spectra and wavelength-ranges in figure 3.1). Then, an auto-correlation FCS experiment for both wavelength ranges was conducted as well as a cross-correlation FCS experiment between the two wavelength ranges. Without the need of a detailed model, the conformation-hypothesis could be verified: as shown in figure 2.4 c), the green-red cross-correlation function exists proving that green and red emission originates from one and the same molecule (albeit not at the same time).

With the existence of a steady-state of conformational dynamics on (PerAcr)₂ proven, the goal was to develop a dynamic model and the corresponding time constants from the FCS results. A way to analytically model the measured correlations curves was derived (cf. table 2.1 for a summary) and different models for the conformational dynamics on the one hand and for the nature of ISO-(PerAcr)₂ on the other hand were tested, cf. figure 2.7. The best fit to the data was achieved assuming the co-existence of two independent emitters in the ISO-(PerAcr)₂ conformation as well as a third, non-fluorescent conformation. In the first case, the fluorescence anti-bunching dip for nearly simultaneous emission in the green auto-correlation curve was nearly half as pronounced as it would have been for only one emitter. The assumption of two emitters is legit, considering the dimeric nature of (PerAcr)₂ and the resemblance of the ISO-(PerAcr)₂ spectra to the monomer spectra. In the second case, the part of the cross-correlation curve dominated by conformational dynamics showed a rise followed by a decay; since for two species, only one decay is theoretically possible, a third species had to be assumed. This was in good agreement with the already existing data hinting at a non-

fluorescent process / species. A non-fluorescent species was thus incorporated into the model and labelled NF-(PerAcr)₂.

The origin of NF-(PerAcr)₂ could not be determined in the scope of publication 2. From the steady-state and time-resolved fluorescence experiments could be determined that its absorption and emission spectra are probably monomer-like. Control experiments eliminated the possibility of NF-(PerAcr)₂ being a triplet or charge-transfer state.

In the scope of publication 2, three dynamically interchanging conformations of (PerAcr)₂ were found and their spectral characteristics were determined along with their conformational dynamics. For the unravelling of the nature of the NF-conformation there was the need for more experimental observables. Time resolved fluorescence anisotropy with its sensitivity to geometric arrangement and orientation was deemed a good way to increase the understanding of this and also of the other two conformations.

3.2.2 Detailed characterisation of (PerAcr)₂ conformations by a combination of time-resolved fluorescence anisotropy and molecular modelling

Consequently, publication 3 incorporates results from time-resolved fluorescence anisotropy experiments on (PerAcr)₂, with detection of the fluorescence signals in the two spectral regions already defined in publication 2. As a first finding, the fluorescence anisotropy decays depend on the detection wavelength, as shown in figure 3.2. As a consequence, a model of these decays needed to treat all (PerAcr)₂ conformations separately with regard to their anisotropy decay. It was also necessary to assume a bi-exponential anisotropy decay to ISO-(PerAcr)₂ to take into account the segmental mobility of the isolated PBIs with respect to the overall complete molecule.

It soon turned out that for a thorough understanding of the experimental results more potent means of modelling were needed as up to that time. Thus, molecular dynamics simulations and modelling were included in the study. As can be seen in figure 3.3 a)-c), the simulations also produced three distinguishable conformations. In the following, the results and analyses concerning the AGG, NF and ISO conformations from the combination of time-resolved fluorescence experiments and molecular simulations and modelling are introduced conformation by conformation.

The simulation results uncovered a conformation in which the two PBIs are stacked co-facially with their distance and orientation in good agreement with former experimental and theoretical results of comparable compounds; consequently, this conformation was identified as AGG-(PerAcr)₂. With respect to the undecylalkyl linker between the dye, the conformation is parallel, meaning that the two PBI-linker interfaces are next to each other (a second, anti-parallel aggregated conformation is discussed below). Concerning the modelling of the measured anisotropy decays, the AGG-conformation was the only point where a refinement of the initial model was necessary: As can be seen in figure 3.2 c), the model could not

completely describe the onset of the measured data. A more complex model (model 2) based on published suggestions about the relaxation processes in PBI stacks [25] was derived (cf. figure 3.4). With this model, the data could be described well, albeit the assumption had to be made that a part of the aggregates (or all aggregates with a certain probability) undergoes a hampered relaxation between excitation and emission of the detected photons. The updated model assumes explicitly that the anisotropy decay of this subset of AGG-(PerAc₂) – dubbed AGG' for distinction – is different from the unhampered case. The results of the fit to the data corroborate this claim: Judging by the corresponding initial anisotropies, AGG-(PerAc₂) is excited in the J-band as well as the H-band by the excitation wavelength used in the experiment, while the discernible signal from AGG'-(PerAc₂) stems solely from excitation into the H-band (cf. table 3.1). Unfortunately, neither the available experimental evidence nor the MD simulations allowed for a further explanation of the hampered relaxation. In the case of AGG-(PerAc₂) MD simulations were used to substantiate claims already made on the basis of the experimental data.

The MD simulations predict also a second aggregated (PerAc₂) conformation, oriented in an anti-parallel way with respect to the position of the PBI-linker interfaces. This conformation is energetically not as favourable when compared to the parallel aggregate (cf. the free energy diagram in fig 3.3 f)). Furthermore, there is a much higher fluctuation in distance and orientation of the two PBIs; and one of the aromatic end-groups of (PerAc₂) is constantly in the direct vicinity of one PBI (cf. figure 3.3 c)). Since those two features are both possible quenching mechanisms, the anti-parallel aggregate has been identified as NF-(PerAc₂). Considering the initial anisotropy of NF-(PerAc₂), it had to be speculated that the effective quenching mechanism is more efficient in aggregates excited into the H-band. In the case of NF-(PerAc₂), only the comparison of simulation and experiment could show that the subtle effect of the symmetry breaking by the undecylalkyl linkers has a big effect on the physical properties of the compound.

Finally, in the case of ISO-(PerAc₂), which was identified with the third “conformation” found in the MD-simulations – over significant periods of time, no aggregation took place in the simulations, cf. figure 3.3d) – the time-resolved anisotropy data served as a direct test of two different models based on the simulation. The processes involved in the absorption and fluorescence in both aggregated conformations (excitation in different bands, relaxation and quenching processes) were not suitable for a modelling of anisotropy decays on the basis of the semi-classical MD simulations alone. But for the ISO conformation it was possible to model anisotropy decays by comparing the trajectory of the orientation of one and the same PBI (cf. equation 3.8). This approach assumes implicitly that fluorescence is emitted from the same PBI that was excited before. The comparison of the model anisotropy decay to the experimental decay showed only a very superficial match, while a similar approach to the anisotropy decay of the PerAc₂ monomer had been more successful (cf. figure 3.SI_1). Consequently, the modelling was refined assuming a probabilistic hopping of between the two PBIs based on an elementary FRET estimation using their time-dependent distance and relative orientation (cf. equations 3.9 to 3.11). The anisotropy decays based on this refined model matched the experimental results to a high degree, especially accounting for the fact that no free parameters were used in the modelling. The comparisons were conducted quantitatively using the results of fits to the data/ the modelled anisotropy decay on the one

hand; on the other hand, the superiority of the hopping model can be directly seen in a qualitative comparison between the measured and modelled anisotropy decays (cf. figure 3.5). Thus, the combination of time-resolved fluorescence anisotropy experiments and modelling based on MD-simulations allowed to prove that energy transfer between isolated PBIs is a relevant mechanism in $(\text{PerAcr})_2$ (and supposedly higher order oligomers resp. polymers, too).

3.2.3 Implications for further research

The studies on $(\text{PerAcr})_2$ presented here establish the following picture of this compound and presumably of other compounds based on the same ingredients and method of preparation (like higher order oligomers resp. polymers and finally even block-copolymers like the ones that originally prompted the studies). As originally designed, aggregation is a dominant feature in the compound, but different than expected, there are “bad” (anti-parallel, NF- $(\text{PerAcr})_2$) and “good” aggregates (parallel, AGG- $(\text{PerAcr})_2$); and for a significant fraction of the time, the PBIs do not aggregate at all (ISO- $(\text{PerAcr})_2$).

The anti-parallel aggregates are heavily quenched and thus a liability if incorporated in organic solar cells or similar devices. Further research could aim on distinguishing between the aforementioned aromatic end-groups or the fluctuations of distance and orientation of the PBIs as the main loss mechanism in these aggregates. As a more direct approach, it could be aimed to find alternatives to aromatic end-groups in the preparation of PerAcr compounds and to limit the length and / or the flexibility of the linkers so that anti-parallel aggregates are avoided.

The parallel aggregates are the prevailing conformation in $(\text{PerAcr})_2$ and behave largely as expected based on similar compounds found in literature: a net blue-shift in absorption is accompanied by a featureless red-shifted fluorescence and a significant increase in fluorescence lifetime. While the observed effect of hindered relaxation seems to be a specialty of this specific sort of compound and tempts the physicist to further investigate its origins, it is possibly not of much relevance in the determination whether PBI-polymers are a candidate for efficient organic solar cells. This is because recent findings imply that large PBI aggregates intrinsically tend to re-localize on a pair of PBIs shortly after excitation, which means that next to the energy-loss due to electronic and vibrational relaxation, the transport of an exciton to the interface of a hypothetical organic solar cell is interrupted. [25] This fact challenges the whole idea of PBI-aggregates as building blocks for solar cells.

A possible way out of this dilemma comes from the third conformation found in $(\text{PerAcr})_2$: in their un-aggregated form, the PBIs in $(\text{PerAcr})_2$ behave much like independent emitters: their absorption and fluorescence spectra as well as their fluorescence lifetime resemble closely their counterpart from the PerAcr monomer. But as this work has shown, they do interact: after excitation, there is a constant hopping of the excitation from one PBI to the other on timescales as short as some tens of picoseconds by a FRET-like homo-energy-transfer mechanism. Compared to the fluorescence lifetime of some nanoseconds this could

mean hundreds to thousands of hops between excitation and emission. This means that possibly good excitation transport properties in combination with a low energy loss could be achieved if this effect was used as the main transport mechanism in an organic solar cell. The main implication of this work is thus to investigate the preparation and characterisation of PBI-polymers that are optimised for resonant energy transfer and actively prevent aggregation.

3.3 Summary

The first publication reports on fluorescence correlation spectroscopy studies on the interaction between CODH and the cytoplasmic membrane of *O. carboxydovorans*. The inherent sensitivity of FCS to the size of the sample particles was exploited to directly prove that the binding of CODH to the cytoplasmic membrane of (CO-grown) *O. carboxydovorans* is specific. Up to that point in time this fact could only be proven rather indirectly.

This study demonstrated the potential of fluorescence spectroscopic methods applied to questions in the field of flavo-enzymes. Further investigations on the mechanism of CODH-binding to the cytoplasmic membrane on the one hand and experiments on ps-timescale processes in CODH on the other had already been prepared. But the lack of the mutated enzyme species required as a reference made a switch of focus – from CODH to (PerAcr)₂ – necessary.

Consequently, the second publication covers the characterisation of (PerAcr)₂ by a combination of spectroscopic techniques. Using an upgraded FCS setup it was possible to discover 3 distinct conformations of (PerAcr)₂ that dynamically interchange on one and the same molecule. Next to the fact that (PerAcr)₂ switches between an isolated and an aggregated state on a μ s-timescale a third, de facto non-fluorescent conformation was found. Steady-state and time-resolved fluorescence spectroscopy delivered excitation- and emission-spectra as well as fluorescence-lifetimes of the fluorescent conformations, whereas the nature of the non-fluorescent state could not be determined.

This led to an additional study with the aim of a more detailed look into the spatial and orientational character of the three (PerAcr)₂ conformations. A combination of streak-camera based time-resolved fluorescence anisotropy and molecular dynamics simulations uncovered a hampered relaxation in the aggregated conformation, identified the non-fluorescent conformation as second, anti-parallel way of aggregation and provided good evidence that in the isolated state a FRET-like hopping of the excitation between the two dyes takes place.

The two publications on (PerAcr)₂ demonstrated that conformations matter in the design of new compounds for organic devices and the usefulness of spectroscopic methods in the corresponding characterisation and model-building. They also provide concrete implications for further development of improved poly-PBI compounds.

4 Publications

The next three sections contain the publications that resulted from this work, in order of appearance. Where applicable, the associated supporting information is shown directly after the main publication. The publications are termed publication 1, 2 and 3 according to the following list:

Publication 1:

F. SPREITLER, C. BROCK, A. PELZMANN, O. MEYER AND J. KÖHLER,
“Interaction of CO Dehydrogenase with the Cytoplasmic Membrane Monitored by
Fluorescence Correlation Spectroscopy”,
ChemBioChem **11**, 2419 – 2423 (2010)

Publication 2:

F. SPREITLER, M. SOMMER, M. THELAKKAT AND J. KÖHLER,
“Conformational dynamics of di-(perylene bisimide acrylate) and its footprints in steady-
state, time-resolved, and fluorescence-correlation spectroscopy”,
Phys. Chem. Chem. Phys. **14**, 7971–7980 (2012)

Publication 3:

F. SPREITLER, M. SOMMER, M. HOLLFELDER, M. THELAKKAT, S. GEKLE AND J. KÖHLER,
“Unravelling the conformations of di-(perylene bisimide acrylate) by combining time-
resolved fluorescence-anisotropy experiments and molecular modelling”,
Phys. Chem. Chem. Phys. **16**, 25959 – 25968 (2014)

5 Bibliography

- [1] F. Spreitler, C. Brock, A. Pelzmann, O. Meyer and J. Köhler, "Interaction of CO Dehydrogenase with the Cytoplasmic Membrane Monitored by Fluorescence Correlation Spectroscopy," *ChemBioChem*, vol. 11, pp. 2419-2423, 2010.
- [2] F. Spreitler, M. Sommer, M. Thelakkat and J. Köhler, "Conformational dynamics of di-(perylene bisimide acrylate) and its footprints in steady-state, time-resolved, and fluorescence-correlation spectroscopy," *Phys. Chem. Chem. Phys.*, vol. 14, p. 7971–7980, 2012.
- [3] F. Spreitler, M. Sommer, M. Hollfelder, M. Thelakkat, S. Gekle and J. Köhler, "Unravelling the conformations of di-(perylene bisimide acrylate) by combining time-resolved fluorescence-anisotropy experiments and molecular modelling," *Phys. Chem. Chem. Phys.*, vol. 16, pp. 25959-25968, 2014.
- [4] J. R. Lakowicz, "Introduction to Fluorescence," in *Principles of Fluorescence Spectroscopy*, 3rd ed., New York, Springer Science+Business Media LLC, 2006.
- [5] J. R. Lakowicz, "Energy Transfer," in *Principles of Fluorescence Spectroscopy*, 3rd ed., New York, Springer Science+Business Media LLC, 2006.
- [6] J. R. Lakowicz, "Quenching of Fluorescence," in *Principles of Fluorescence Spectroscopy*, 3rd ed., New York, Springer Science+Business Media LLC, 2006.
- [7] A. Eisfeld and J. S. Briggs, "The J-band of organic dyes: lineshape and coherence length," *Chemical Physics*, no. 281, pp. 61-70, 2002.
- [8] A. Eisfeld and J. S. Briggs, "The J- and H-bands of organic dye aggregates," *Chemical Physics*, no. 324, pp. 376-384, 2006.
- [9] J. R. Lakowicz, "Instrumentation for Fluorescence Spectroscopy," in *Principles of Fluorescence Spectroscopy*, 3rd ed., New York, Springer Science+Business Media LLC, 2006.
- [10] C. C. R. Hofmann, *Energy and Electron Transfer in Organic Donor-Acceptor Systems*, Bayreuth, 2010.
- [11] T. Pflock, *Energy Transfer Between Light-Harvesting Complexes*, Bayreuth, 2012.
- [12] J. R. Lakowicz, "Time-Resolved Protein Fluorescence," in *Principles of Fluorescence Spectroscopy*, 3rd ed., New York, Springer Science+Business Media LLC, 2006.
- [13] J. Widengren and Ü. Mets, "Conceptual Basis of Fluorescence Correlation Spectroscopy and Related Techniques as Tools in Bioscience," in *Single Molecule Detection in Solution: Methods and Applications*, C. Zander, J. Enderlein and R. A. Keller, Eds., Weinheim, Wiley-VCH, 2002.
- [14] J. R. Lakowicz, "Fluorescence Anisotropy", "Time-Dependent Anisotropy Decays", "Advanced Anisotropy Concepts," in *Principles of Fluorescence Spectroscopy*, 3rd ed., New York, Springer Science+Business Media LLC, 2006.

- [15] O. Meyer and H. G. Schlegel, "Carbon monoxide:methylene blue oxidoreductase from *Pseudomonas carboxydovorans*," *Journal of Bacteriology*, vol. 141, pp. 74-80, 1980.
- [16] H. Theorell, "Preparation in pure state of the effect group of yellow enzymes," *Biochemische Zeitschrift*, vol. 275, pp. 344-6, 1935.
- [17] S. M. H. Christie, G. W. Kenner and A. R. Todd, "Nucleotides. Part XXV. A synthesis of flavin-adenine dinucleotide," *Journal of the Chemical Society*, pp. 46-52, 1954.
- [18] H. Cypionka and O. Meyer, "Carbon Monoxide-Insensitive Respiratory Chain of *Pseudomonas carboxydovorans*," *Journal of Bacteriology*, vol. 156, pp. 1178-1187, 1983.
- [19] H. Dobbek, L. Gremer, R. Kiefersauer, R. Huber and O. Meyer, "Catalysis at a dinuclear [CuSMo(=O)OH] cluster in a CO dehydrogenase resolved at 1.1-Å resolution.," *Proceedings of the National Academy of Sciences of the United States of America*, vol. 99, pp. 15971-6, 2002.
- [20] M. Rohde, F. Mayer, S. Jacobitz and O. Meyer, "Attachment of CO dehydrogenase to the cytoplasmic membrane is limiting the respiratory rate of *Pseudomonas carboxydovorans*," *FEMS Microbiology Letters*, vol. 28, pp. 141-144, 1985.
- [21] S. Jacobitz and O. Meyer, "Removal of CO dehydrogenase from *Pseudomonas carboxydovorans* cytoplasmic membranes, rebinding of CO dehydrogenase to membranes, rebinding of CO dehydrogenase to respiratory activities.," *Journal of Bacteriology*, vol. 171, pp. 6294-6299, 1989.
- [22] F. Spreitler, *unpublished results*.
- [23] M. Somer, S. M. Lindner and M. Thelakkat, "Microphase-Separated Donor-Acceptor Diblock Copolymers: Influence of HOMO Energy Levels and Morphology on Polymer Solar Cells," *Advanced Functional Materials*, vol. 17, pp. 1493-1500, 2007.
- [24] S. Hüttner, M. Sommer and M. Thelakkat, "n-type organic field effect transistors from perylene bisimide block copolymers and homopolymers," *Applied Physics Letters*, vol. 92, p. 093302, 2008.
- [25] A. Schubert, M. Falge, M. Kess, V. Settels, S. Lochbrunner, W. T. Strunz, F. Würthner, B. Engels and V. Engel, "Theoretical Analysis of the Relaxation Dynamics in Perylene Bisimide Dimers Excited by Femtosecond Laser Pulses," *The Journal of Physical Chemistry*, vol. 118, pp. 1403-1412, 2014.

Danksagung

Bettina,

Danke dass du da bist.

Dass du immer zu mir gehalten hast.

Dass du getreten und getröstet, festgehalten und geschoben hast.

Danke dass du da bist.

Ich liebe dich.

Jürgen, bitte nimm mir diese letzte Unverschämtheit bei der Dankespriorisierung nicht übel.

Ich danke dir für die Möglichkeit, mit dir forschen zu dürfen, für die Diskussionen und die Hilfe bei der Themenverlagerung. Für deine Treue und Ausdauer in den Jahren, in denen ich nicht mehr vor Ort war. Danke.

Astrid, Michael und Stephan, Danke für die tolle und vertrauensvolle Zusammenarbeit.

Chris, du bist der beste Diplomand, den ich je hatte. Und ein guter Freund. Danke.

Streak-Kompetenz-Team: Tobi, Christiane. Danke. Fürs. Zusammen. Dranbleiben.

Dominique, Danke für Physik, Freundschaft, vielfältige Hobbies.

Evelyn, Danke fürs Kümmern.

An alle anderen, die in meiner Bayreuther Zeit mit mir gelernt, geforscht, gegrübelt, geschraubt, gestritten, gelacht, Mittag gegessen und Weihnachten gefeiert haben, die mir geholfen haben und unter mir zu leiden hatten: Ich zähle euch nicht einzeln auf, weil ich Angst habe jemand zu vergessen. Ihr wisst, wer ihr seid. Danke.

Mama und Papa, Brigitte und Bernd, Danke für alles.

Paul, Jakob und Lotte, schön dass es euch gibt.

Erklärung

Hiermit erkläre ich, dass ich die vorliegende Arbeit selbständig verfasst und keine anderen als die angegebenen Quellen und Hilfsmittel benutzt habe. Die Arbeit wurde in gleicher oder ähnlicher Form keiner anderen Prüfungsbehörde zur Erlangung eines akademischen Grades vorgelegt. Ich habe noch keinen promotionsversuch unternommen.

Des Weiteren erkläre ich, dass ich Hilfe von gewerblichen Promotionsberatern bzw. -vermittlern oder ähnlichen Dienstleistern weder bisher in Anspruch genommen habe noch künftig in Anspruch nehmen werde.

Aalen, den 1.4.16

Florian Spreitler